Using Wheel Slippage for Improved Maneuverability of 4 Wheel Steering Vehicles

Erdem Ata and A. Bugra Koku

Abstract In the domain of land vehicles, the researches which focus on the subject of slippage mostly develop methods for detecting and avoiding slippage or compensating for slippage. Even when slippage is considered as a potential advantage, this is mostly researched for high speeds. This paper proposes a method that uses slippage as an advantage even at low speeds. This is achieved by using the nonholonomic properties of a 4WS (4 wheel steering) vehicle with independent front and rear drives. It is experimentally shown that controlled low speed slippage can be advantegous for certain tasks by comparing the vehicle behavior to a similar 2WS (2 wheel steering) vehicle which cannot leverage slippage.

Keywords 4WS · 2WS · AWS · Ackerman steering · Wheel slip · Drift · Maneuverability

1 Introduction

Autonomous ground vehicles (AGVs) can be used in crowded spaces such as offices and homes, or on challenging terrains. They can be used for carrying items in an office or in a warehouse and carrying out rescue missions on challenging terrains. Uneven terrains or unpaved off-road scenarios may require high maneuverability to carry out certain tasks.

There are different vehicle structures to achieve different amounts of maneuverability. The most common vehicle structure used in daily life is 2WS (2 wheel steering) cars. While adding more complexity to the vehicle structure, 4WS (4 wheel steering) cars provide higher maneuverability by allowing a smaller turning radius [8]. Both of these structures are designed to mostly avoid slippage and some researches assume no-slip conditions while modeling these vehicles [7]. Some outdoor vehicles such as

E. Ata (✉) · A. B. Koku
Department of Mechanical Engineering, Middle East Technical University, Ankara, Türkiye
e-mail: ataerdem@gmail.com

METU-ROMER, Middle East Technical University, Ankara, Türkiye

G. L. Conte and O. Sename (eds.), *Proceedings of the 11th International Conference on Mechatronics and Control Engineering*, Lecture Notes in Mechanical Engineering,
https://doi.org/10.1007/978-981-99-6523-6_12

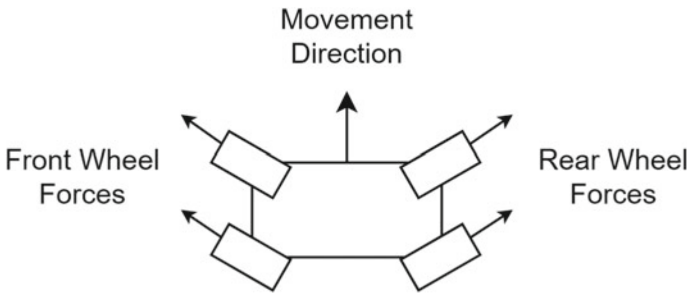

Fig. 1 An example case where the vehicle can move sideways using wheel slippage

tanks may utilize differential drives with no steering to provide arbitrarily small turning radii. However, all the movements that can be executed by differential drive vehicles involve slippage. The maneuverabilities of these vehicle structures have been extensively studied so far [5, 6, 10, 13, 14].

Wheel slippage is not desired for various reasons. On one hand slippage accumulates error in dead reckoning, on the other hand, it decreases controllability of vehicles. Hence, slippage in general is not a desired state. However, it may be useful to force these vehicles to slip for certain tasks. While vehicles with 4WS-4WD with independent front and rear drives and differential drives can start slippage at low speeds, a 2WS vehicle with Ackerman steering cannot.

In this paper, it is hypothesized and later shown that using 4WS with independent drives for front and rear wheels, one can control the vehicle to slip in an arbitrary direction without requiring prior maneuvers. As an example, consider the case shown in Fig. 1 where a 4WS vehicle steers at the opposite directions with the front and rear wheels while driving the front and rear wheels in the opposite directions. This actuation may cause the vehicle to drift sideways if controlled properly.

Although the results of excessive slippage may have adverse effects on wheels in everyday usage, using slippage only when it is completely necessary may allow cars to execute maneuvers that are otherwise harder or impossible such as fitting in tight parking spots or making very sharp maneuvers in crowded places. Since most 4WD electric cars already use independent electric motors for front and rear drives, the proposed structure is somehow similar to existing cars. However, controlling 4 inputs, 2 steering angles and 2 drive speeds, manually is a considerably more difficult task compared to driving a regular car. Therefore, the control of slippage needs to be automated for such applications in order to get the maximum benefit from wheel slippage.

In order to automate the controlled slippage to enhance maneuverability, we present a proper mathematical model for the proposed vehicle structure in the next section. While the starting point is the commonly used bicycle model, many additions and modifications are added to the model in order to make it more suitable for the case where the vehicle slips. The nonlinear model of the vehicle is then linearized to utilize linear state space methods.

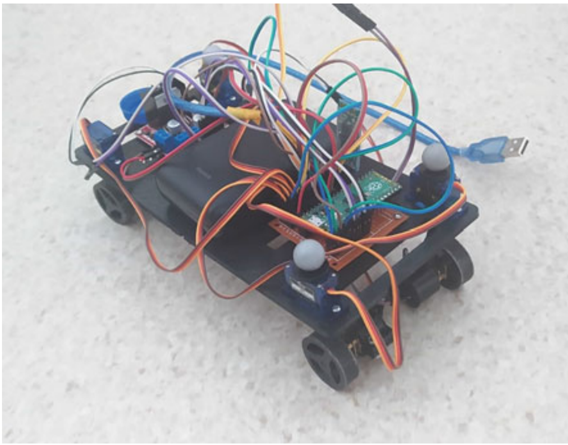

Fig. 2 Small scale prototype

In the third section, two different control methods are discussed. The first one is a relatively naive approach that allows the user to directly use the coordinates of the vehicle as reference states using LQR. The second control method allows the user to control the vehicle to follow a certain path to reach to a given coordinate. In order to enable the vehicle to follow a certain path, a linear transformation is applied to the states of the system using the output matrix. Then, the controller's parameters are tuned in order to prioritize staying on the given line.

Finally, the proposed method is applied to the real life small scale prototype shown in Fig. 2. The feedback for the controller is provided using a Vicon optical motion tracking system. Using the same controller structure, a 2WS and a 4WS vehicle with independent drives (proposed structure) is compared. In order to compare the performances of different vehicles, their performance on following a relatively challenging trajectory is considered.

2 Mathematical Model

The mathematical model can be inspected in three parts: wheel forces, friction moment and input limits. After considering those points, a non-linear dynamic model is created using Kane's method and sympy mechanics module on Python. To utilize linear state space methods, the model is linearized around the instantaneous state at any time step using the Jacobian method. This requires the evaluation of system matrix and input matrix at each time step while keeping the linear approximation fairly accurate at any time.

Plant inputs are selected as steering angles (θ_f, θ_r) and angular velocities of the wheels (ω_f, ω_r). The states are selected as the position of the vehicle (x, y),

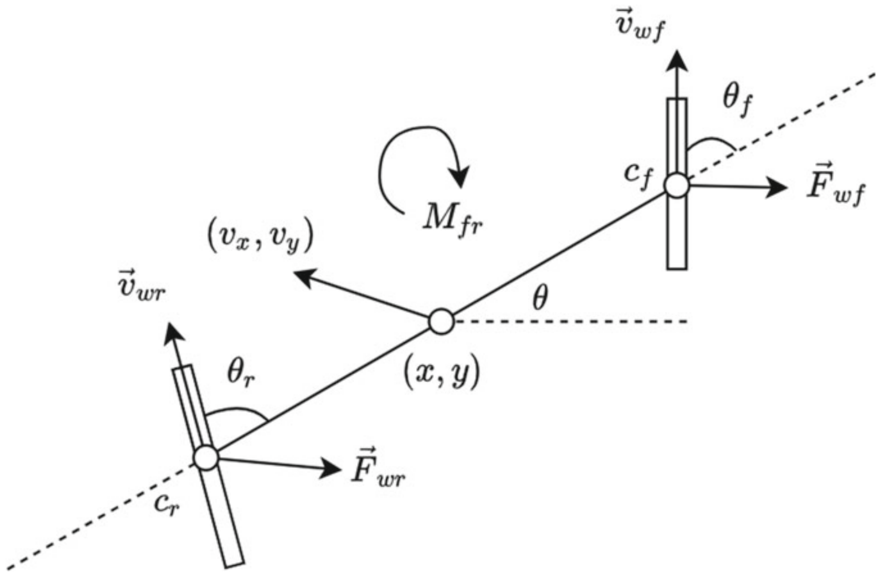

Fig. 3 Mathematical model

orientation of the vehicle with respect to the x axis (θ), the velocity of the vehicle (v_x, v_y) and the angular velocity of the vehicle (ω) respectively as shown in (1) and Fig. 3.

$$\mathbf{x} = \begin{bmatrix} x \\ y \\ \theta \\ v_x \\ v_y \\ \omega \end{bmatrix} \tag{1}$$

2.1 Wheel Forces

For the mathematical model, the vehicle is considered to be a rigid body in a planar space with 2 wheels (front and rear) attached as shown in Fig. 3. The friction between the wheels and the ground is assumed to be viscous. Although this assumption is clearly counter-intuitive, it results in a simple (i.e. less non-linear) mathematical model. It is hypothesized and observed in the experiments that the inaccuracy is not significant at tested speeds.

Under the viscous friction assumption, the force that is applied on the vehicle by a single wheel can be expressed with the following equation.

$$\vec{F}_{w,i} = c_i(\vec{v}_{w,i} - \vec{v}_{c,i}), \quad i = f, r \tag{2}$$

where c_i is the viscous friction coefficient between the wheel and the ground, $\vec{v}_w$ is the velocity which is dictated by the wheel and $\vec{v}_c$ is the velocity of the wheel center with respect to the ground.

For a given wheel, $\vec{v}_w$ can be expressed in terms of the inputs θ_i and ω_i.

$$\vec{v}_{w,i} = r\omega_i(\cos(\theta_i + \theta)\hat{\boldsymbol{\imath}} + \sin(\theta_i + \theta)\hat{\boldsymbol{\jmath}}), \quad i = f, r \tag{3}$$

where θ_i is the steering angle and ω_i is the angular velocity by which the wheel is driven. The subscript i is used to denote whether the wheel is front or rear.

2.2 Friction Moment

When the rotation of the vehicle around the front wheel alone is considered, the assumption of no friction due to the rotation can be acceptable. However, when there are 2 front wheels, in order to account for the friction caused by the rotation of the vehicle around the center of the front wheels, one has to introduce an extra moment to the bicycle model. This moment is assumed to be proportional to the angular velocity of the vehicle and the friction coefficient. It is also affected by the distance between the front wheels. Then the additional friction moment can be represented by the following expression.

$$\vec{M}_{fr} = -d\vec{\omega}(c_r + c_f) \tag{4}$$

where $\vec{M}_{fr}$ is the additional friction moment, d is the distance between the front wheels and $\vec{\omega}$ is the angular velocity of the vehicle.

2.3 Input Limits

Both the steering angle and the angular velocity of the wheels are limited to certain ranges. Due to the non-linearity of the system, simply clipping the controller outputs before feeding them into the plant would not work. The limits of these variables should be represented in the mathematical model.

In order to achieve that, 2 variables which are expressed with the following equations are introduced.

$$\omega_i = l_\omega \tanh(\omega_i^{initial}), \quad i = f, r \tag{5}$$

$$\theta_i = l_\theta \tanh(\theta_i^{initial}), \quad i = f, r \tag{6}$$

If the plant inputs are selected as $\omega_i^{initial}$ and $\theta_i^{initial}$, then the absolute values of steering angle and the angular velocity of the wheels will be limited to l_ω and l_θ respectively.

3 Control Method

Using the linear quadratic regulator (LQR) method, the states can be directly controlled to achieve a desired state. For a linear system, LQR method optimizes the expression given in (7). However, that does not put any constraint on the path that will be followed. For most tasks that require the vehicle to move to a certain location, a specific path should be followed. Using a proper output matrix, the vehicle can be controlled to follow a line with a specific speed. For more complicated paths, it is possible to approximate the path with line segments.

$$\int_0^\infty \mathbf{x}^T \mathbf{Q} \mathbf{x} + \mathbf{u}^T \mathbf{R} \mathbf{u} \, dt \tag{7}$$

For both methods, two important tricks are used. Firstly, since the controller is allowed to instantly change the steering angles in the mathematical model, this causes a discrepancy between the model and reality. Similarly, the driving angular velocity of the wheels cannot be instantly changed. To resolve this issue, the controller's steering output is forced to be pseudo-continuous by limiting the change between time steps. Secondly, when the controller decides to suddenly change the steering angles and apply a certain angular velocity to the wheels, before the new steering angle is applied, the wheels may start to turn. This causes an unintended action to be executed. In order to overcome this problem, the angular velocities are significantly reduced when a sudden steering angle change is detected.

3.1 State Control

While using LQR directly on the states (with unit output matrix) allows one to move the vehicle from a given position and orientation to another, the priorities cannot be properly defined for the controller. An example path is shown in Fig. 4.

As the example suggests, the vehicle is controlled from the origin to the desired arbitrary position, $(0.3, 0.07)$ m, successfully. However, the optimum decision of the LQR does not enable one to control the path. The $\mathbf{Q}$ matrix of the LQR for this example is given in (8).

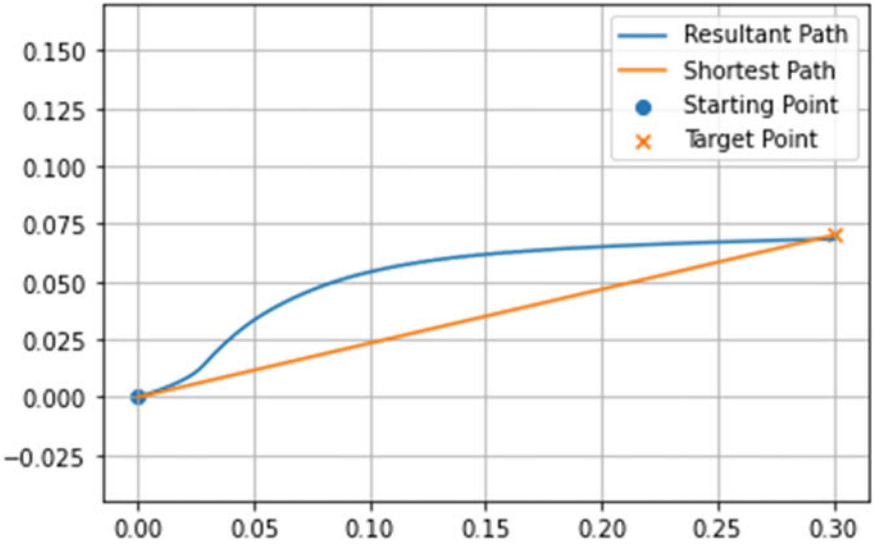

Fig. 4 The resultant path of controlling with unit output matrix in a mathematical simulation

$$\mathbf{Q} = \begin{bmatrix} 1 & 0 & 0 & 0 & 0 & 0 \\ 0 & 1 & 0 & 0 & 0 & 0 \\ 0 & 0 & 1 & 0 & 0 & 0 \\ 0 & 0 & 0 & 0 & 0 & 0 \\ 0 & 0 & 0 & 0 & 0 & 0 \\ 0 & 0 & 0 & 0 & 0 & 0 \end{bmatrix} \tag{8}$$

3.2 Output Control

To overcome the issue of not being able to control the path, a suitable output matrix can be defined. The purpose is to define a line that connects the initial and reference positions of the vehicle and use one of the states as the deviation from this line. The same transformation can be applied to the velocities.

Let the line that connects the initial position and the reference position be defined by the equation $ax + by = c$. Choosing the output matrix and reference state as

$$\mathbf{C} = \begin{bmatrix} a & b & 0 & 0 & 0 & 0 \\ a' & b' & 0 & 0 & 0 & 0 \\ 0 & 0 & 1 & 0 & 0 & 0 \\ 0 & 0 & 0 & a & b & 0 \\ 0 & 0 & 0 & a' & b' & 0 \\ 0 & 0 & 0 & 0 & 0 & 1 \end{bmatrix} \tag{9}$$

$$\mathbf{r} = \begin{bmatrix} c \\ c' \\ \theta_{ref} \\ 0 \\ c_{vel} \\ \omega_{ref} \end{bmatrix} \tag{10}$$

enables one to prioritize the error in a new coordinate system. To make the transformed coordinate system an orthogonal coordinate system with the reference position as the origin and the new y axis as the line to be followed, a', b', c' can be chosen as follows.

$$a' = b \tag{11}$$

$$b' = -a \tag{12}$$

$$c' = bx_r - ay_r \tag{13}$$

Let the goal position be $\vec{p}_r = x_r\hat{\imath} + y_r\hat{\jmath}$, and the initial position be $\vec{p}_i = x_i\hat{\imath} + y_i\hat{\jmath}$. The desired velocity can be calculated using the expression

$$c_{vel} = b\vec{g} \cdot \hat{\imath} - a\vec{g} \cdot \hat{\jmath} \tag{14}$$

where $\vec{g}$ is the unit vector in the direction of the desired movement.

$$\vec{g} = (\vec{p}_r - \vec{p}_i)/|\vec{p}_r - \vec{p}_i| \tag{15}$$

Using the described output matrix, the first two error components represent e_1 and e_2 in Fig. 5.

Using the output matrix $\mathbf{C}$ and reference input $\mathbf{r}$, the path given in Fig. 6 can be obtained.

The vehicle is controlled between the same initial and final positions. However, in this example, the errors are properly prioritized to control the vehicle on a line. The $\mathbf{Q}$ matrix of the LQR for this example is given in (16).

$$\mathbf{Q} = \begin{bmatrix} 10 & 0 & 0 & 0 & 0 & 0 \\ 0 & 0.1 & 0 & 0 & 0 & 0 \\ 0 & 0 & 1 & 0 & 0 & 0 \\ 0 & 0 & 0 & 1 & 0 & 0 \\ 0 & 0 & 0 & 0 & 0.1 & 0 \\ 0 & 0 & 0 & 0 & 0 & 0 \end{bmatrix} \tag{16}$$

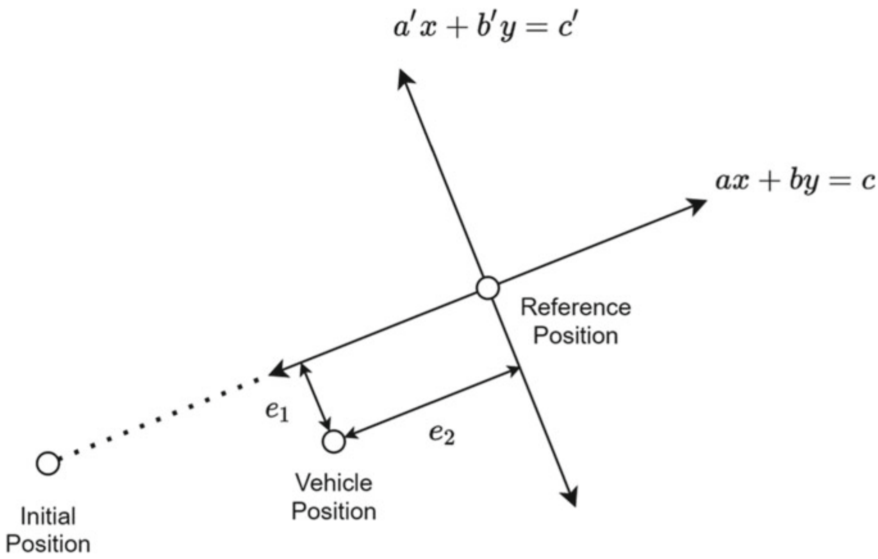

Fig. 5 The transformed coordinate system and the error components

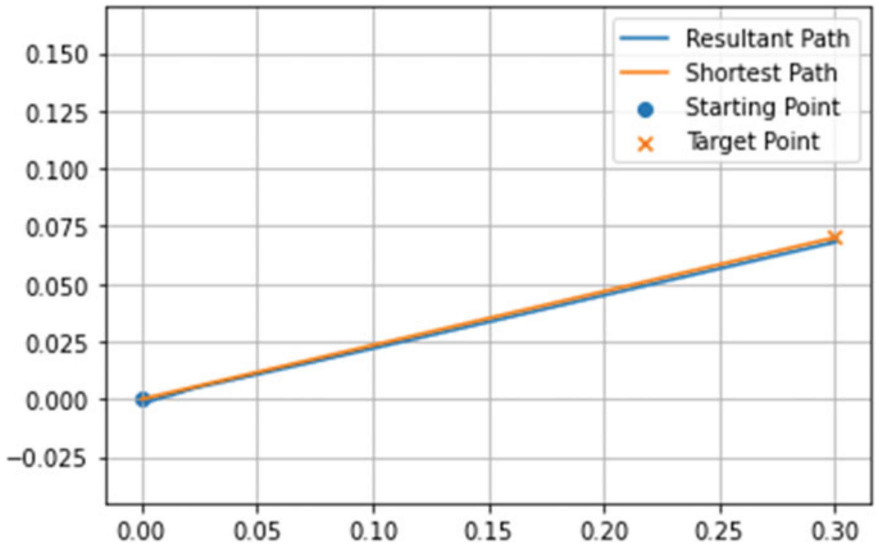

Fig. 6 The resultant path of controlling with the described output matrix in a mathematical simulation

4 Experimental Results

4.1 Setup

The proposed 4WS, 4WD vehicle structure is tested on a prototype vehicle with state feedback from a Vicon optical motion capture system. The structure is compared to a commonly used 2WS vehicle structure in terms of trajectory tracking performance. Equation (17) describes the cost metric.

$$C = \int_{0}^{t_f} |\vec{x}_t(t) - \vec{x}_v(t)|\, dt \tag{17}$$

where t_f is the time when the end point is reached, $\vec{x}_t(t)$ is the position the vehicle has to be on at the time t and $\vec{x}_v(t)$ is the position of the vehicle at the time t.

As a test case, the vehicles are initially positioned at the origin with 0° angle (i.e. facing east). Then, the vehicles are controlled to the position (0, 0.4) m targeting approximately 3.33 cm/s in the direction of the target.

Since the control of a 2WS vehicle requires long term planning, the movement is divided into several parts. For each part, a similar controller is used and different controller parameters are selected.

For the 2WS vehicle, three long term strategies are used. The first one involves the vehicle to make a smooth movement towards the end of the trajectory but this requires the vehicle to considerably deviate from the line. For the second strategy, the vehicle executes 2 maneuvers to change its angle before moving towards the end point. The last strategy involves 4 maneuvers however, this causes the vehicle to delay and increases the trajectory tracking cost.

The maneuvers simply involve the vehicle being controlled to a specific angle until a certain deviation from the desired path is reached. This corresponds to a case where the vehicle has to move in a narrow hallway since deviating too much from the middle of the hallway is not possible.

For the 4WS vehicle, 2 different reference input, priority pairs are used. The first one involves the vehicle to be controlled at 0° while tracking the trajectory. In the given figures, this mode is called "Full Slip" since the vehicle has to always slip during the motion. The second mode involves the vehicle to be controlled to 1.37 radians during the motion. Once the angle target is reached, the vehicle does not have to slip for the rest of the motion. Since movement towards the target without slippage can be achieved in a relatively wide angle range, the angle priority of the controller is selected to be somehow lower compared to the first mode.

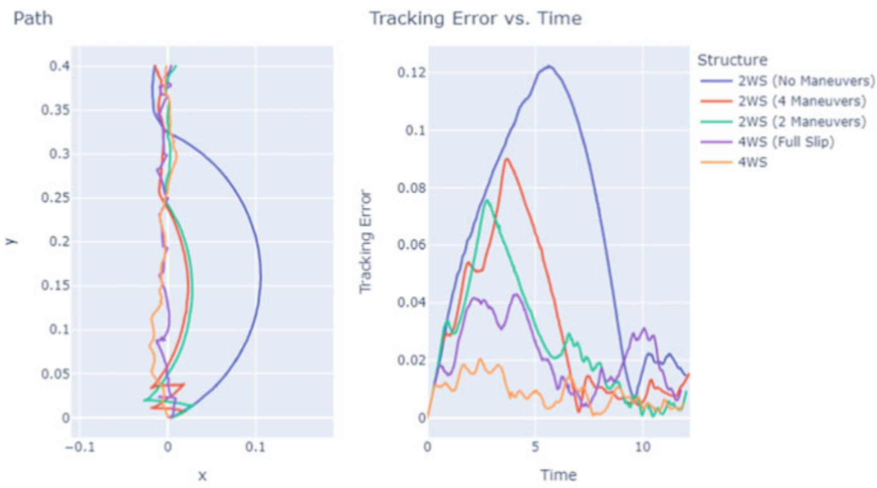

(a) Paths that are followed by the vehicles

(b) Trajectory errors of the vehicles through time

Fig. 7 Paths and trajectory errors

4.2 Results

The paths that are followed by the vehicles and the deviation from the trajectory in the best trial for each are given in Fig. 7a, b respectively.

Using (17) for the given trials, the costs of different structures and modes are given in Table 1. This result shows that making more than 2 maneuvers only causes the 2WS vehicle to delay further. This means that it is not necessary to increase the number of maneuvers any further.

The trajectory tracking errors defined by the metric given in (17) are given in Table 1.

The maximum error in terms of the angle was less then 12° when the 4WS vehicle was controlled to 0° during the motion.

An animation of the movements of different structures in the experiment are given in this video.

Table 1 Costs of different structures and modes

Mode	Cost
2WS (No maneuvers)	0.767
2WS (4 maneuvers)	0.386
2WS (2 maneuvers)	0.319
4WS (Full slip)	0.260
4WS	0.103

Two videos of simulations are given in video 1 where the vehicle follows a narrow hall while maintaining a desired orientation and video 2 where the vehicle parks in a difficult spot.

A recording of a real life experiment is given in this video.

4.3 Discussion

Figure 7a suggests that the proposed vehicle model can maintain a velocity towards the target with a relatively smaller deviation from the shortest path. However, the baseline 2WS vehicle has to either considerably deviate from the desired path or make multiple maneuvers causing it to lag.

The results given in Table 1 demonstrate that the proposed structure can perform significantly better even when it is forced to stay at angle which requires slippage. When the angle requirement is relaxed, a further significant improvement can be obtained for the proposed structure.

5 Conclusion

In this work, it is shown that slippage at low speed can be advantageous while tracking a challenging trajectory. A warehouse robot which has to make sharp maneuvers in a crowded space or a regular car which is trying to parallel park in a tight spot may need to follow a challenging trajectory which may might be possible to follow without slippage.

It is shown that using the proposed structure and the controller, the vehicle can be forced to slip in a desired direction without prior maneuvers. It is also important to note that the proposed structure can avoid slippage unless it is necessary. Therefore the adverse effects of excessive slippage can be avoided when it is not necessary to slip.

Even though a similar amount of maneuverability may be reached by complex wheel structures such as omni wheels, the proposed method demonstrates that it can be done with simpler wheels.

Acknowledgements METU-ROMER supported this work by providing access several to manufacturing methods, electronic components and the motion tracking system Vicon. This work would not have been possible without the support of METU-ROMER.

References

1. Deepak SV, Naresh C, Hussain SA (2012) Modelling and analysis of alloy wheel for four wheeler vehicle. Int J Mech Eng Robot Res 1(3):72–80
2. Choudhari DS (2014) Four wheel steering system for future. Int J Mech Eng Robot Res 3(4):383–387
3. Saxena S, Kumar V, Luthra SS, Kumar A (2014) Wheel steering systems (4WAS). Int J Mech Eng Robot Res Special Issue 1(1):213–218
4. Rajasekar R, Pranavkarthik KP, Prashanth R, Kumar SS (2013) Design and fabrication of staircase climbing wheelchair. Int J Mech Eng Robot Res 2(2):320–323
5. Jhino S, Lincol V, Josue L, Junior Q, Carlos M (2018) Maneuverability study of a vehicle with rear wheel steering. Mech. Mach. Sci. 54:559–567. https://doi.org/10.1007/978-3-319-67567-1_52/FIGURES/7
6. Mondal K, Wallace B, Rodriguez AA (2020) Stability versus maneuverability of non-holonomic differential drive mobile robot: focus on aggressive position control applications. In: CCTA 2020—4th IEEE conference on control technology and applications, pp 388–395. https://doi.org/10.1109/CCTA41146.2020.9206155
7. Xu G, Wang D (2006) Full state tracking of a four-wheel-steering vehicle based on output tracking control strategies. In: 9th international conference on control, automation, robotics vision, 2006, ICARCV ’06. https://doi.org/10.1109/ICARCV.2006.345154
8. Kang J, Yoo J, Yi K (2011) Driving control algorithm for maneuverability, lateral stability, and rollover prevention of 4WD electric vehicles with independently driven front and rear wheels. IEEE Trans. Veh. Technol. 60(7):2987–3001. https://doi.org/10.1109/TVT.2011.2155105
9. Bayar G, Bergerman M, Konukseven EI, Koku AB (2016) Improving the trajectory tracking performance of autonomous orchard vehicles using wheel slip compensation. Biosyst Eng 146:149–164. https://doi.org/10.1016/J.BIOSYSTEMSENG.2015.12.019
10. Hafizah N et al (2016) Modelling and control strategies in path tracking control for autonomous ground vehicles: a review of state of the art and challenges. J Intell Robot Syst 86(2):225–254. https://doi.org/10.1007/S10846-016-0442-0
11. Taghia J, Wang X, Lam S, Katupitiya J (2017) A sliding mode controller with a nonlinear disturbance observer for a farm vehicle operating in the presence of wheel slip. Auton. Robot. 41(1):71–88. https://doi.org/10.1007/S10514-015-9530-4/TABLES/4
12. Yin GD, Chen N, Wang JX, Chen JS (2010) Robust control for 4WS vehicles considering a varying tire-road friction coefficient. Int J Automot Technol 11(1):33–40. https://doi.org/10.1007/S12239-010-0005-5
13. Pilisiewicz J, Kaczyński R (2017) Geometric analysis of maneuverability performance for vehicles with two steering axles. Transp Probl 12(2):43–52. https://doi.org/10.20858/tp.2017.12.2.5
14. Choi MW, Park JS, Lee BS, Lee MH (2008) The performance of independent wheels steering vehicle(4WS) applied Ackerman geometry. In: 2008 International Conference on Control, Automation, Systems ICCAS, 2008, pp 197–202. https://doi.org/10.1109/ICCAS.2008.4694549
15. Bayar G, Koku AB, Konukseven EI (2015) Dynamic modeling and parameter estimation for traction, rolling, and lateral wheel forces to enhance mobile robot trajectory tracking. Robotica 33(10):2204–2220. https://doi.org/10.1017/S0263574714001386
16. Kane T, Levinson D (1985) Dynamics, theory and applications. McGraw-Hill, New York